Controlled Assembly of 1,4-Phenylenedimethanethiol Molecular Nanostructures

Hadi M. Zareie, Andrew M. McDonagh, Jonathan Edgar, Michael J. Ford, Michael B. Cortie, Matthew R. Phillips*

Institute for Nanoscale Technology, University of Technology Sydney, PO Box 123, Broadway NSW 2007, Australia.

Hadi.zareie@uts.edu.au

RECEIVED DATE (to be automatically inserted after your manuscript is accepted if required according to the journal that you are submitting your paper to)

1,4-Phenylenedimethanethiol Nanostructures

We present here the first high-resolution scanning tunneling microscope images showing that 1,4-phenylenedimethanthiol forms mono- and multilayers on gold(111) substrates under particular solution deposition conditions. The high-resolution images show that the deposition conditions strongly influence the type of surface structure formed. The molecular structures were also probed using molecular etching techniques as well as through deposition and imaging of gold nanoparticles. The current-voltage (I/V) characteristics of the multilayer structures are significantly different to those of monolayers. For the first time, scanning electron microscopy experiments were used to investigate the homogeneity of larger surface areas of the surface structures.

Introduction

The study of electrical conduction through molecules has attracted significant attention.[1-7] A number of configurations have been used to create molecular junctions between metal contacts.[4,8-10] Commonly, molecules under investigation have been attached to gold surfaces using thiol groups. Structures made from 1,4-phenylenedimethanethiol[11] (Figure 1) have been used extensively in this area.[12-14] The 1,4-phenylenedimethanethiol molecules stand upright on gold surfaces anchored by one of the two thiol groups,[15] leaving one thiol group free to bind to a second metallic contact. Gold nanoparticles, for example, have been used for this purpose.[16-21] Recently, Pugmire *et al*[15] concluded that 1,4-phenylenedimethanethiol can form multilayered structures on gold surfaces under certain conditions, with implications for any subsequent molecular conductivity experiments. Rifai and Morin[22] showed that an oxidative mechanism can be utilized to form multilayers of 1,4-phenylenedimethanethiol on gold by the formation of disulfide bonds between unbound thiol groups of surface-bound molecules and thiol groups on molecules from solution. We present here the first high-resolution STM images showing that 1,4-phenylenedimethanthiol can form both mono- and multilayers on gold substrates under particular solution deposition conditions.

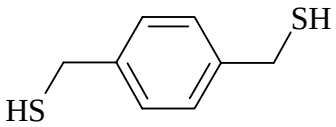

Figure 1. 1,4-phenylenedimethanethiol

Experimental Section

Materials. 1,4-phenylenedimethanethiol and gold nanoparticles (5 nm diameter, 0.01 % as $HAuCl_4$) were purchased from Aldrich and used as received. Gold (111) films (150 nm thick on mica) were purchased from Molecular Imaging (Arizona, USA) and flame annealed before use.

Preparation of molecular structures on gold. Gold films (~ 5 mm x 5 mm) were immersed in 2 mL of a 1 mM solution of 1,4-phenylenedimethanethiol in deoxygenated absolute ethanol under a nitrogen atmosphere. The containers were sealed, and placed in the dark for periods ranging from 8 to 48 h at either room temperature or 55 °C. The substrates were then removed from the solution, rinsed liberally with absolute ethanol, and dried with a slow stream of nitrogen gas. To prepare multilayered structures, the procedure above was used to form SAMs of 1,4-phenylenedimethanethiol on gold (24 h immersion time at room temperature) and the sample was subsequently re-immersed in a 0.1 mM solution of 1,4-phenylenedimethanethiol in absolute ethanol and incubated at 55°C for 12 hours before being rinsed liberally with ethanol and dried with nitrogen gas. Gold/SAM/gold nanoparticle structures were prepared by first preparing a SAM of 1,4-phenylenedimethanethiol on gold (24 h immersion time at room temperature) and then immersing the sample in a gold particle solution for 24 hours at room temperature. The sample was then rinsed with ethanol and dried under a stream of nitrogen gas.

X-ray photoelectron spectroscopy. Data were acquired using a Kratos Axis ULTRA X-ray Photoelectron Spectrometer incorporating a 165mm hemispherical electron energy analyser. The incident radiation was monochromatic Al X-rays (1486.6eV) at 150W (15kV, 10ma). Survey (wide) scans were taken at an analyzer pass energy of 160eV and multiplex (narrow) high resolution scans at 20eV. Survey scans were carried out over 1200-0eV binding energy range with 1.0eV steps and a dwell time of 100ms. Narrow high-resolution scans were run with 0.1ev steps and 250ms dwell time. Base pressure in the analysis chamber was 1.0×10^{-9} torr and during sample analysis 1.0×10^{-8} torr.

Secondary ion mass spectrometry. Secondary ion mass spectrometry data were acquired using a Kratos PRISM Time-of-Flight Secondary Ion Mass Spectrometer. The primary ion source was 69Ga, which produced a beam of 25 KeV ions. The analysis area was approximately 0.15 mm x 0.15 mm.

Scanning electron microscopy. Scanning electron microscope (SEM) images were obtained using a LEO Supra 55VP SEM (Zeiss) equipped with an in-lens secondary electron detector. Images were manipulated using Scanning Probe Image Processor (SPIP) software and colour brightness has been added to the images using Adobe Photoshop to enhance discrimination of the fine detail.

Scanning tunneling microscopy and spectroscopy. STM images were acquired using a Nanosurf EasyScan system under ambient conditions. STM piezoelectric scanners were calibrated laterally, with graphite(0001) and Au(111), and vertically, using the height of the Au(111) steps (2.2 Å). The STM tip was prepared from Pt/Ir wire cut under ambient conditions. All images were acquired in a constant-current mode. Typical imaging conditions are bias voltages of ± 0.2 to ±1 V and a tunneling current of 3 pA to 1 nA. Images shown are raw data unless stated otherwise. Images were manipulated with the Scanning Probe Image Processor (SPIP) software. Contrast-enhanced images were obtained by applying a correlation averaging procedure to analyze repeat molecular units and by a applying low-pass filter. The relative tunneling spectroscopy was determined from I-V measurements. The relevant surface area was imaged before and after STS measurements to ensure no tip or sample alterations occurred during the experiment. Images of the same area showed no changes after STS with the exception of a small lateral drift of the sample between the two scans.

Results and Discussion

Preparation and Characterization of SAMs. SAMs of 1,4-phenylenedimethanethiol were prepared on gold by liquid-solid phase assembly. Gold substrates were immersed in a solution of 1,4-phenylenedimethanethiol at room temperature for periods of 8, 24, and 48 h under oxygen-free conditions. Additionally, a sample was prepared at 55 °C for 48 h. Each sample was imaged using scanning tunneling microscopy. X-ray photoelectron spectroscopy, time-of-flight secondary ion mass spectrometry, and scanning electron microscopy experiments were performed on samples prepared at room temperature with 24 h immersion time.

The S 2*p* x-ray photoelectron spectrum of a SAM prepared under these conditions has features matching those reported in detail by Pugmire *et al*.[15] In that report, the authors concluded that the S 2*p* XPS spectrum consisted of signals assigned to gold-bound thiol, gold-bound atomic S, and unbound molecular thiol or disulphide. This is consistent with the molecule being bound to the gold substrate by one of the two available thiol groups, and also with the reported formation of multi-layered structures.

Secondary ion mass-spectrometry (SIMS) experiments were performed on a sample prepared by the same method (see Supporting Information for negative and positive ion spectra). SIMS experiments on SAMs of 1,4-phenylenedimethanethiol have been previously reported by others,[23] although only data up to m/z 190 were reported. In the current work, measurements up to m/z 750 were performed. The negative ion spectrum contains a signal corresponding to the molecular ion, indicating 1,4-phenylenedimethanethiol is present on the gold surface. Signals assigned to $[Au\text{-}SH]^-$ and $[Au(SH)_2]^-$ fragments are also observed together with higher masses, which were not able to be unambiguously assigned.

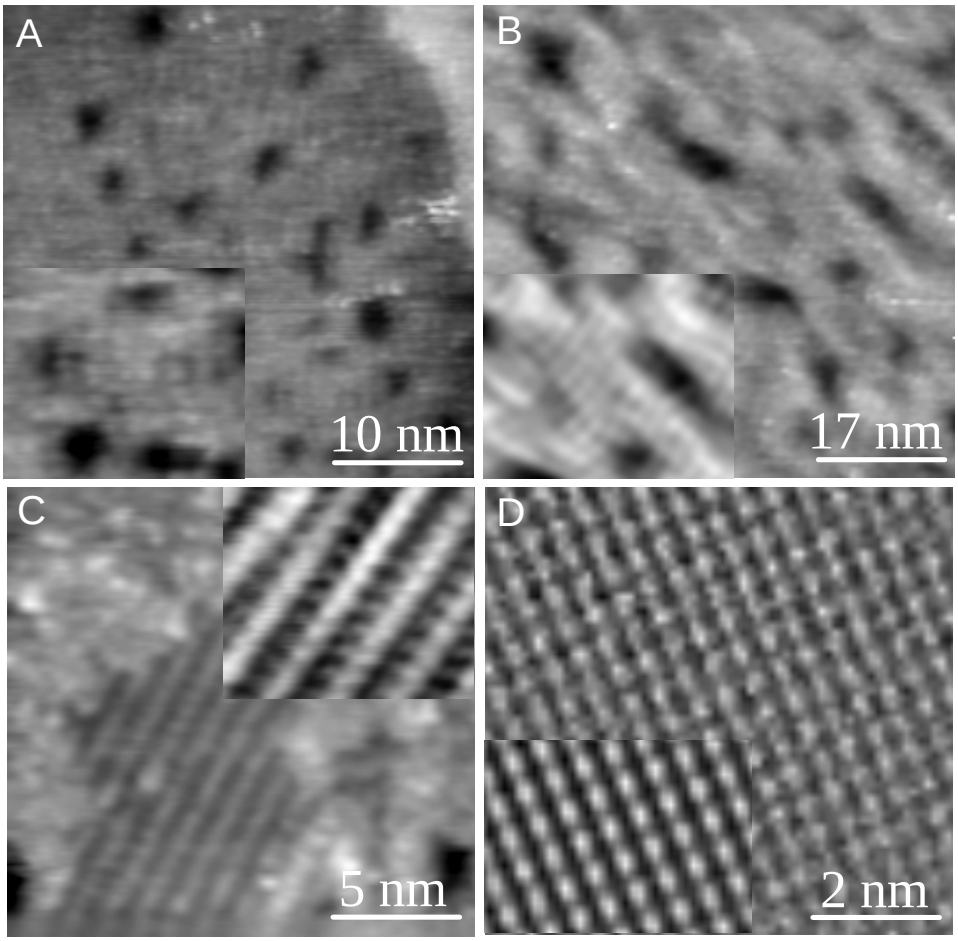

Figure 2. STM images of assemblies of 1,4-phenylenedimethanethiol on gold(111). (A) after 24 h at room temperature (Inset: higher magnification image 12 x 11 nm) (B) after 48 h at room temperature (Inset: higher magnification image 27 x 22 nm), (C) after 48 h at 55 ^{o}C (Inset: higher magnification image, 4.8 x 4.2 nm) and (D) after 8 h room temperature (image is low-pass filtered) (Inset: 4 x 3.5 nm). Inset images are contrast enhanced.

The structures of self-assembled films were studied at atomic resolution using scanning tunneling microscopy. Figure 2A shows a representative sample after 24 h immersion at room temperature. The image shows many 2.4 ± 0.2 Å deep 'vacancy islands'. These monoatomic depressions are similar in number density, size, and shape to those found in other thiol-bound SAMs on gold.[24] Between the vacancy islands, the monolayer is composed of generally unorganized molecules. Figure 2A (inset)

shows a contrast-enhanced section of the image formed by application of a correlation averaging procedure (see Experimental Section). Features of approximately 6 Å diameter are apparent and are consistent with individual 1,4- phenylenedimethanethiol molecules.

Figure 2B shows an STM image of a sample after 48 h immersion in a solution maintained at room temperature. Again, the typical "vacancy islands" are evident but some molecular ordering is also observed. The contrast-enhanced image, Figure 2B (inset), shows domains of molecular rows with an inter-row separation (peak to peak) of 1 ± 0.2 nm.

Figure 2C shows an STM image of a sample after 48 h immersion in a solution maintained at 55 ºC. Larger structured domains are apparent. The contrast-enhanced image, Figure 2C (inset) is shown at higher magnification. The separation between the rows is 1 ± 0.6 nm, consistent with the data obtained for the samples assembled for 48 h at room temperature. We ascribe the brighter spots in this image to the phenyl rings in 1,4-phenylenedimethanethiol and the smaller gray spots to S atoms. The distance between the centres of two adjacent phenyl rings within a row is 0.49 ± 0.08 nm. The domains yield a nearly rectangular lattice with $\alpha = 9.8 \pm 0.5$ Å, $\beta = 5.1 \pm 0.1$ Å, $\gamma = 82 \pm 0.2^{o}$.

Surprisingly, immersion of gold substrates in solutions of 1,4-phenylenedimethanethiol for shorter time intervals such as 8 to 10 h at room temperature resulted in the formation of structures of the type shown in Figure 2D. Analysis of the Fourier transform of the image in Figure 2D reveals a rectangular surface net with lattice constants of $\alpha = 3.9 \pm 0.3$ Å, $\beta = 3.7 \pm 0.1$ Å, $\gamma = 88 \pm 0.2^{o}$. It is important to note that because STM analysis covers relatively small areas, no generalizations about the entire surface morphologies are made. However, the first high-resolution STM images of 1,4-phenylenedimethanethiol structures on gold shown here indicate that molecular ordering is highly dependent on the time and temperature of sample preparation.

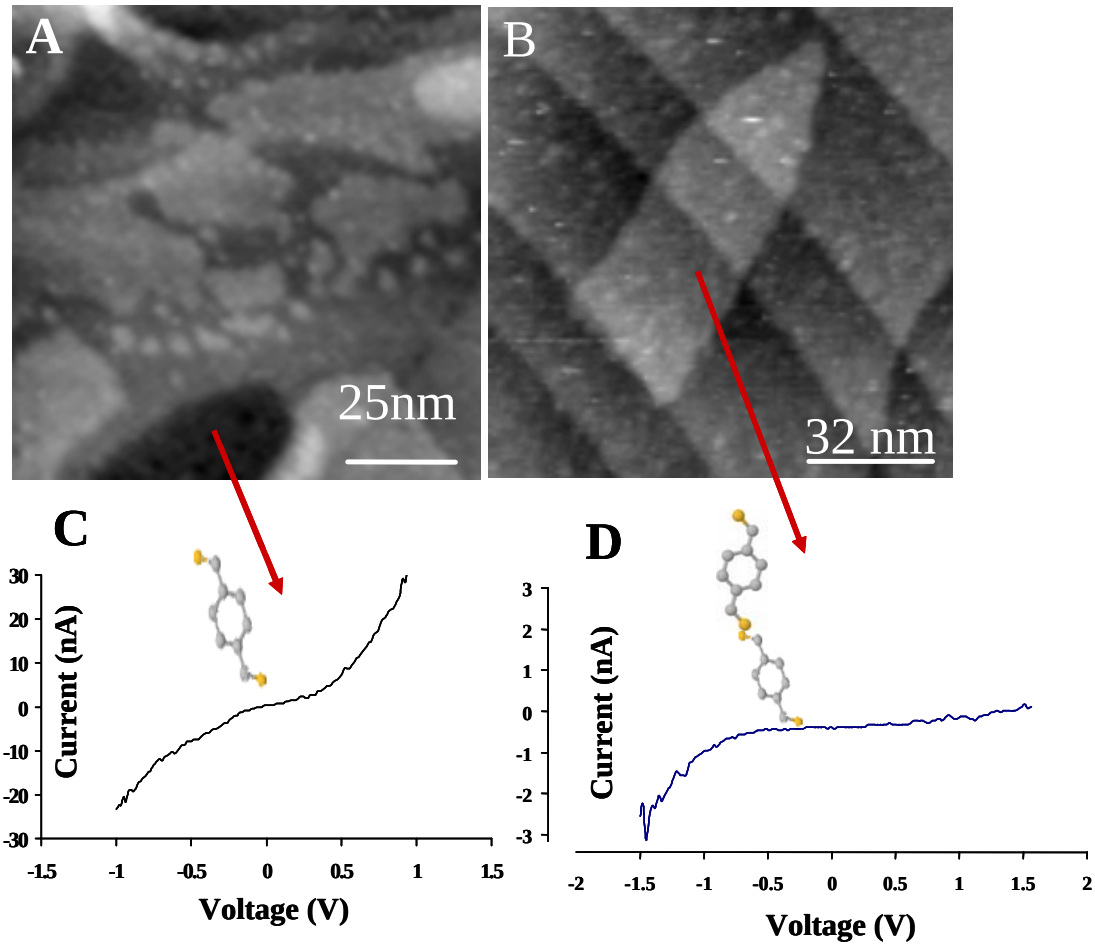

Figure 3. *I-V* characteristics of single and double layers of 1,4- phenylenedimethanethiol on gold(111). (A and B) are two different images showing double layer regions, (C) STS of a single layer region, and (D) STS of a double layer region.

STM images of multilayer structures. Pugmire *et al*[15] reported that preparation of SAMs of 1,4-phenylenedimethanethiol SAMs could result in structures containing multilayers. These may be formed by disulfide linkages between the free thiol groups of molecules attached to gold and thiols from unbound molecules (from solution). Disulfides are often the first oxidation products of thiol compounds[25] so we performed experiments whereby SAMs formed by the procedure outlined in the previous section (24 h immersion time, room temperature) were re-immersed in a solution of 1,4-phenylenedimethanethiol without any precautions to exclude air. Figure 3 shows STM images of samples prepared by this procedure. In both images, the steps associated with gold domain boundaries

are visible. Figure 3A contains a number of features not observed in the SAMs shown in Figure 2. Although steps and vacancy islands are observed in some regions, which correspond to a single-layer structure (dark area), islands of molecules are visible that we assign to a multilayered structure. Line profiles taken across these images are consistent with a second layer of 1,4-phenylenedimethanethiol molecules. The formation of this second layer is dependent on sample preparation; in our hands whenever the sample is prepared without rigorous exclusion of oxygen we observe regions that correspond to multilayer structures.

Scanning tunneling spectroscopy experiments yielded an I/V curve for a monolayer region (Figure 3C) showing a characteristic sigmoidal form while the curve measured on a double layer region (Figure 3D) is significantly different.

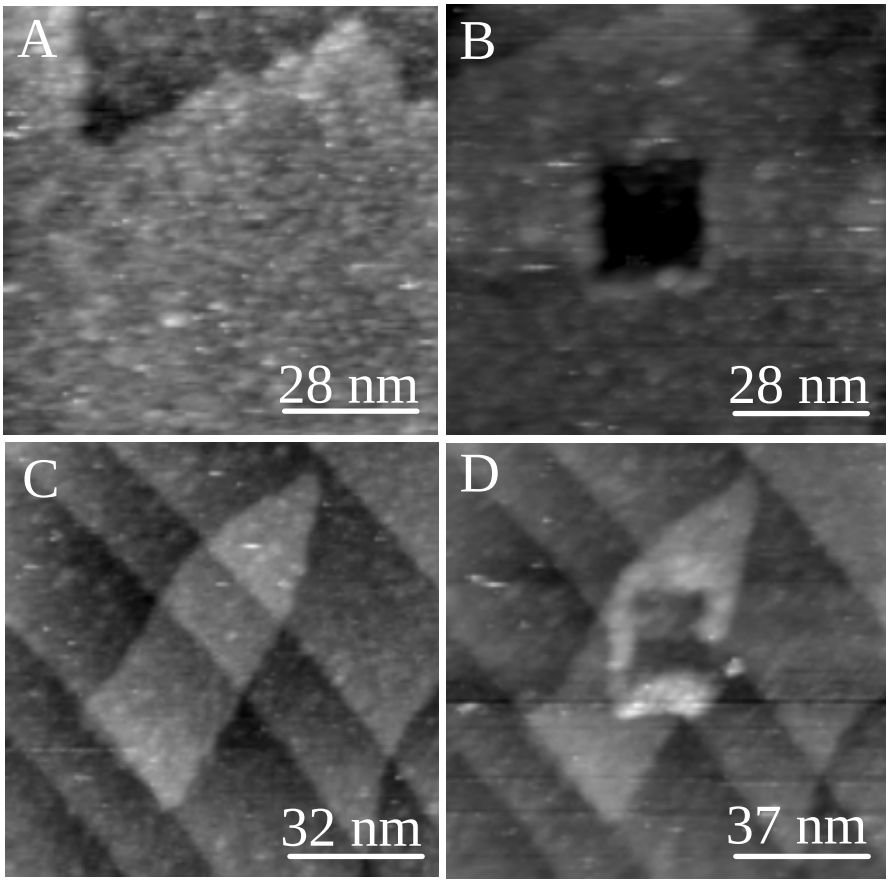

Figure 4. (A and C) STM images of 1,4- phenylenedimethanethiol film coated on Au/mica (A single layer and C double layer). (B) Same area shown in (A) after etching. (D) Same area shown in (C) after etching.

Molecular etching experiments[26] were performed to further probe the single and multilayer structures. In this experiment, the molecular layers are first scanned under normal imaging conditions (V_{bias} = 1 V and $I_{tunneling}$ = 1 nA). Pits were then etched by bringing the STM tip close to the surface using parameters V_{bias} = 10 mV and $I_{tunneling}$ = 10 nA and scanning a 20 x 20 nm area for 30 s at 0.75 s per line. Increasing the scan area to 50 x 50 nm and scanning under normal imaging parameters allowed inspection of the etched pits.

Figure 4A shows a monolayer structure before etching. Figure 4B shows the same area after etching of the 1,4-phenylenedimethanethiol SAM. A pit of area 20 x 20 nm is clearly visible. Similarly,

Figure 4C shows a multilayer structure before etching. Figure 4D shows the sample after etching and again, a pit of area 20 x 20 nm is visible. We observed that continuous scanning with V_{bias} = 1 V and $I_{tunneling}$ = 1 nA caused removal of most of the loosely bound material as reported by others.[27] Line profiles taken across the etched pits on the samples shown in Figure4 B and D indicate an apparent pit depth[28] of 0.48 and 0.47 nm, respectively. This suggests that in both cases only a monolayer of 1,4-phenylenedimethanethiol has been removed although no conclusions may be drawn about the precise height of the layers. Furthermore, inspection of the etched pit in the multilayer sample shows features corresponding to the underlying molecules of the surface bound layer.

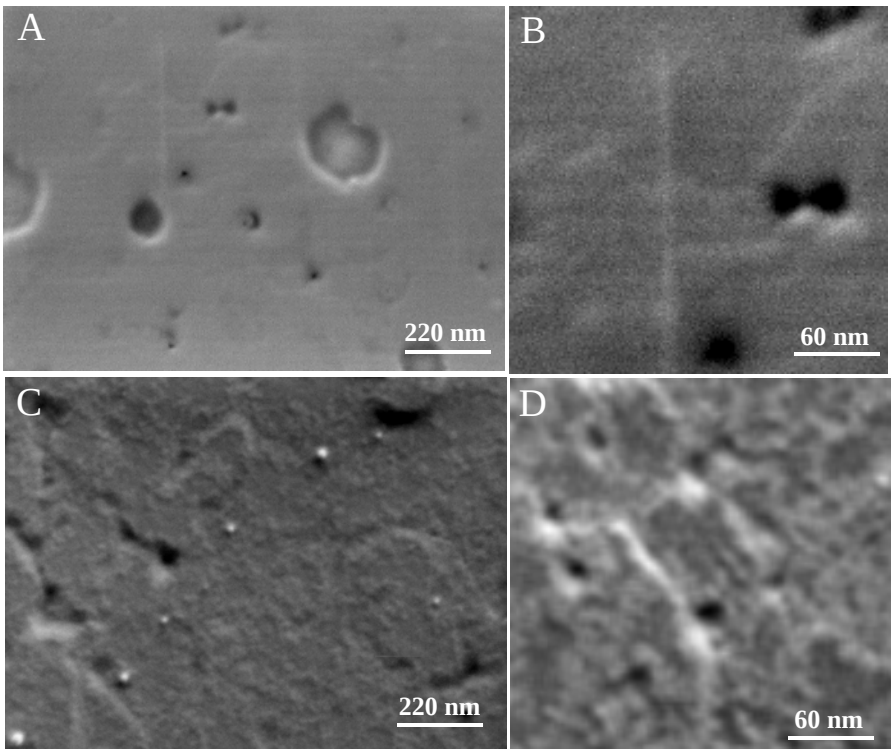

Figure 5. In-lens secondary electron scanning electron microscopy images. (A): bare gold (111), (B) image A processed using a low-pass filter, (C) 1,4-phenylenedimethanethiol SAM on gold prepared at room temperature for 24 h, (D) image C processed using a low-pass filter.

Scanning electron microscopy. Because STM can image only a relatively small area, we performed SEM experiments to investigate the homogeneity of larger surface areas. A representative in-lens secondary electron (SE) SEM image of a bare gold (111) surface is shown in Figure 5A. Boundaries between gold (111) domains and 20 nm pit defects in the gold film are visible. A virtually featureless flat surface is observed within each gold (111) domain. An in-lens SE SEM image of a SAM of 1,4-phenylenedimethanethiol self-assembly on gold (111) (prepared by 24 h immersion at room temperature) is shown in Figure 5C. This SE image reveals a highly textured surface together with the gold domain boundaries and pit defects. The spatial variation of the SE signal, due to the presence of the SAM, is accentuated by applying equivalent image processing procedures together with a low pass filter to both the bare gold surface (Figure 5B) and the SAM on gold surface (Figure 5D). Full interpretation of the SE contrast is difficult as it results from a complex combination of effects arising from differences in the SE yield between the gold substrate and the SAM, differences in the number of molecular layers, changes in the gold work function due to the presence of the molecules and electron beam induced charging-related phenomena. However, SE images show that the 1,4-phenylenedimethanethiol SAM is not homogenous over each of the gold (111) domains. Interestingly, these results suggest that SE imaging can be used to rapidly establish the presence and distribution of the SAM over a large area of specimen.

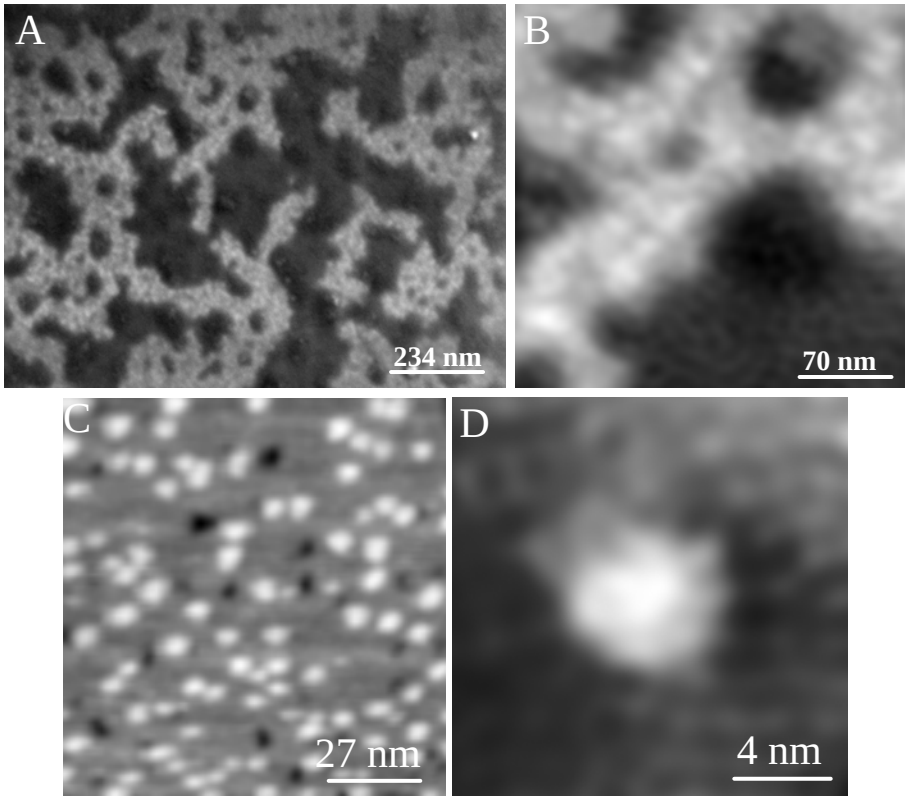

Figure 6. SEM and STM images of 5 nm gold particles on **1**,4-phenylenedimethanethiol SAMs. (A and B) are in-lens SE micrograph. (C and D) are STM images of the nanostructure

To further probe the surface structure, gold nanoparticles (5 nm) were deposited onto a 1,4-phenylenedimethanethiol SAM. Figure 6A and B shows in-lens SE images of the gold (111) / SAM / gold particle structure. Aggregates of gold nano-particles form networks of bright pathways 20 to 200 nm wide that contain ~ 50 nm diameter nano-particle free areas. At higher magnification the individual 5 nm gold nanoparticles can be clearly observed within the pathways (Figure 6B), which appear bright because the entire surface of each gold nano-particle emits secondary electrons. The edges of the gold nano-particle aggregate pathways tend to follow the boundaries of the areas of low SE emission, which are in some cases related to pits in the gold (111) substrate. However, the density of dark features in gold (111) / SAM / gold particle structure is significantly larger than the density of pit defects in the bare gold (111) substrate.

Figure 6C shows an STM image confirming the surface-bound gold nanoparticles have diameters in the range of ~6-8 nm. In Figure 6D, both single gold nanoparticles and the underlying 1,4-phenylenedimethanethiol molecules are visible.

Conclusions

Detailed scanning tunneling microscopy images of self-assembled structures of 1,4-phenylenedimethanthiol molecules on gold(111) have been presented for the first time. The STM data indicate that this molecule can self-organize on gold under particular solution deposition conditions. SAMs of 1,4-phenylenedimethanthiol can exist in different phases. Analysis of STM images shows two different unit cell configurations with each formed under particular conditions. Multilayer SAMs were prepared by a controlled process and imaged with STM. Single layers from the multilayer could be etched using standard STM techniques. Scanning tunneling spectroscopy revealed different electronic behaviour between the single and double layers. Gold nanoparticles could be deposited on 1,4-phenylenedimethanthiol SAMs by solution techniques. Finally, the gold/SAM and gold/SAM/nanoparticle structures were investigated by in-lens electron microscopy for the first time to show regional differences across areas of SAMs.

Acknowledgement. We thank the Australia Research Council for financial assistance and the Microstructural Analysis Unit at the University of Technology Sydney for support with scanning electron microscopy. We also thank Dr. Barry J Wood from the Brisbane Surface Analysis Facility for XPS experiments and Dr. Bill Gong from the School of Chemistry at the University of New South Wales for SIMS experiments.

Supporting Information Available. X-ray photoelectron spectra, secondary-ion mass spectra, and details of STM calibration.

References

[1] Dadosh, T.; Gordin, Y.; Krahne, R.; Khivrich, I.; Mahalu, D.; Frydman, V.; Sperling, J.; Yacoby, A.; Bar-Joseph, I. *Nature* **2005**, *436*, 677.

[2] Joachim, C.; Ratner, M. A. *Proc. Natl. Acad. Sci. USA* **2005**, *102*, 8801.

[3] Flood, A. H.; Stoddart, J. F.; Steuerman, D. W.; Heath, J. R. *Science* **2005**, *306*, 2055.

[4] James, D. K.; Tour, J. M. *Chem. Mater.* **2004**, *16,* 4423.

[5] Nitzan, A.; Ratner, M. A.; *Science* **2003**, *300*, 1384.

[6] Robertson, N.; McGowan, C. A. *Chem. Soc. Rev.* **2003**, *32*, 96.

[7] Joachim, C.; Gimzewski, J. K.; Aviram. A. *Nature* **2000**, *408,* 541.

[8] Xu, B.; Tao, N. J. *Science* **2003**, *301*, 1221.

[9] Chen, J.; Reed, M. A.; Rawlett, A. M.; Tour, J.M. *Science* **1999**, *286,* 1550.

[10] Reed, M. A.; Zhou, C.; Muller, C. J.; Burgin, T. P.; Tour, J. M. *Science* **1997**, *278*, 252.

[11] We use here the IUPAC nomenclature (see http://www.iupac.org/general/FAQs/ns.html) but draw the readers' attention to the large number of names used for this molecule including the Chemical Abstracts Index name**,** 1,4-benzenedimethanethiol, as well as other names; *p*-xylene-α,α'-dithiol, α,α'-dimercapto-*p*-xylene, α,α'-*p*-xylenedithiol, 1,4-benzenebis(methanethiol), 1,4-bis(mercaptomethyl)benzene, 1,4-xylylenedithiol, and *p*-xylylenedithiol.

[12] Andres, R. P.; Bein, T.; Dorogi, M.; Feng, S.; Henderson, J. I.; Kubiak, C. P.; Mahoney, W.; Osifchin, R. G.; Reifenberger, R. *Science* **1996,** *272*, 1323.

[13] Dorogi, M.; Gomez, J.; Osifchin, R.; Andres, R. P.; Reifenberger, R. *Phys. Rev. B* **1995,** *52*, 9071.

[14] Xiao, X.; Xu, B.; Tao, N. J. *Nano Lett.* **2004**, *4*, 267.

[15] Pugmire, D. L.; Tarlov, M. J.; van Zee, R. D.; Naciri, J. *Langmuir* **2003**, *19*, 3720.

[16] Ishizuka, K.; Suzuki, M.; Fujii, S.; Akiba, U.; Takayama, Y.; Sato, F.; Fujihira, M. *Jap. J. Appl. Phys.* **2005**, *44,* 5382.

[17] Joo, S. W.; Han, S. W.; Kim, K. *J. Phys. Chem. B* **1999**, *103,* 10831.

[18] Murty, K. V. G. K.; Venkataramanan, M.; Pradeep, T. *Langmuir* **1998**, *14,* 5446.

[19] Sbrana, F.; Parodi, M. T.; Ricci, D.; Di Zitti, E.; Natale, C.; Thea, S. *Mater. Sci. Eng.* **2002**, *B96,* 193.

[20] Liu, J.; Lee, T.; Janes, D. B.; Walsh, B. L.; Melloch, M. R.; Woodall, J. M.; Reifenberger, R.; Andres, R. P. *Appl. Phys. Lett.* **2000**, *77*, 373.

[21] Vandamme, N.; Snauwaert, J.; Janssens, E.; Vandeweert, E.; Lievens, P.; Van Haesendonck, C. *Surf. Sci.* **2004**, *558,* 57.

[22] Rifai, S.; Morin, M. *J. Electroanal. Chem.* **2003**, *550*, 277.

[23] Pradeep, T.; Evans, C.; Shen, J.; Cooks, R. G. *J. Phys. Chem. B* **1999**, *103,* 5304.

[24] Love, J. C.; Estroff, L. A.; Kriebel, J. K.; Nuzzo, R. G.; Whitesides, G. M. *Chem. Rev.* **2005**, *105,* 1103.

[25] Kohli, P.; Taylor, K. K.; Harris, J. J.; Blanchard, G. J. *J. Am. Chem. Soc.* **1998**, *120,* 11962.

[26] Kim, Y-T.; McCarley, R. L.; Bard, A. J. *Langmuir* **1993**, 9*,* 1941.

[27] Kim, Y-T.; Bard, A. J. *Langmuir* **1992**, *8*, 1096.

[28] Bumm, L. A.; Arnold, J. J.; Dunbar, T. D.; Allara, D. L.; Weiss, P. S. *J. Phys. Chem. B* **1999**, *103,* 8122.